

MICROCOPY RESOLUTION TEST CHART
NATIONAL BUREAU OF STANDARDS-1963-A

AD A 098000

REPORT DOCUMENTATION PAGE		READ INSTRUCTIONS BEFORE COMPLETING FORM
1. REPORT NUMBER NRL Memorandum Report 4493	2. GOVT ACCESSION NO. AD-A098080	3. RECIPIENT'S CATALOG NUMBER
4. TITLE (and Subtitle) A NUMERICAL STUDY OF THE NANOSECOND AND SUBNANOSECOND PERFORMANCE OF GEKKO XII-MODULE	5. TYPE OF REPORT & PERIOD COVERED Interim report on a continuing NRL problem.	6. PERFORMING ORG. REPORT NUMBER
		8. CONTRACT OR GRANT NUMBER(s)
7. AUTHOR(s) R. H. Lehmberg and J. M. McMahon	9. PERFORMING ORGANIZATION NAME AND ADDRESS Naval Research Laboratory Washington, D.C. 20375	
11. CONTROLLING OFFICE NAME AND ADDRESS U.S. Department of Energy Washington, D.C. 20545	10. PROGRAM ELEMENT, PROJECT, TASK AREA & WORK UNIT NUMBERS 47-0859-0-1	
	12. REPORT DATE April 23, 1981	
14. MONITORING AGENCY NAME & ADDRESS (if different from Controlling Office)	13. NUMBER OF PAGES 28	
	15. SECURITY CLASS. (of this report) UNCLASSIFIED	
16. DISTRIBUTION STATEMENT (of this Report) Approved for public release; distribution unlimited.		15a. DECLASSIFICATION/DOWNGRADING SCHEDULE
17. DISTRIBUTION STATEMENT (of the abstract entered in Block 20, if different from Report)		
18. SUPPLEMENTARY NOTES		
19. KEY WORDS (Continue on reverse side if necessary and identify by block number) Laser modelling Glass laser model Comparison with shiva		
20. ABSTRACT (Continue on reverse side if necessary and identify by block number) A numerical study is conducted to examine the performance potential of the GEKKO XII-Module, a phosphate glass laser system currently under development at Osaka University. The study shows that with appropriate modifications, this system should produce peak powers up to 3.6 TW/beam in a 50 psec pulse, and 2-2.5 kJ/beam in a 1 nsec pulse. The similarity between the GEKKO XII-Module and Shiva beam line configurations suggests that a phosphate glass retrofit of Shiva could produce nanosecond pulse energies up to 50kJ.		

A NUMERICAL STUDY OF THE NANOSECOND AND
SUBNANOSECOND PERFORMANCE OF GEKKO XII-MODULE

1. Introduction

The GEKKO XII laser at Osaka University will ultimately be a twelve beam, 20 kJ, 40 TW system design for laser fusion studies.¹ Recently, Osaka University scientists reported on the short pulse performance of the prototype module of this laser, which is called GEKKO XII-Module, quoting an output of up to 3.4 TW/beam before beam breakup was encountered.^{2,3} The GEKKO XII-Module performance is of especial interest to the U.S. ICF program because the components are similar to those in the Shiva laser at Lawrence Livermore National Laboratory⁴ - with the significant difference that LGH-7 phosphate laser glass is used rather than a silicate laser glass. The performance of this laser should therefore provide data on the performance to be expected from Shiva when it is retrofitted with phosphate glass as part of the Nova upgrade.

In this report, we summarize the results of a numerical investigation of the expected performance of the GEKKO XII-Module laser at nanosecond and subnanosecond pulsewidths. The configuration and amplifier (small signal) performance were as specified by the Osaka laser group.¹ The large signal behavior was calculated using the NRL laser amplifier code KARL, plus a spatial filter transmission algorithm similar to that used to model the present performance of Shiva. The Osaka claim of 3.4 TW/beam in a short pulse is reasonable; however, the reported configuration is not a particularly good choice for nanosecond operation, as coating damage would be expected at slightly above 1000J/beam. Various reconfiguration

Manuscript submitted February 10, 1981.

choices and passive optics modifications were examined to alleviate this problem, and with a reasonably optimum strategy, outputs of 1800-2000J/beam appear possible. Addition of a second twenty cm amplifier to each beam would raise the output to about 2500J/beam.

2. GEKKO XII-Module Configuration

The GEKKO XII-Module consists of various preamplifiers followed by a 5-10 cm beam telescope/spatial filter; a 10 cm disc amplifier; a Faraday rotator package; another 10 cm disc amplifier; a 10-15 cm spatial filter telescope; a 15 cm disc amplifier; a Faraday Rotator package; a 15-20 cm spatial filter; a 20 cm disc amplifier; a Faraday Rotator package.¹ A final lens was assumed at the end of the chain as an initial element of a relay telescope/beam expander before the target optics. Figure 1 is the schematic diagram, and Figure 2 shows a recent picture of the installation, with the oscillator and preamplifier section in the center, and the first test arm on the right hand side.

In the computer studies, the performance of components reported by the Osaka group was used where the information was available;¹ where such information was not available, the specifications of the equivalent Shiva component were used.⁴ Exact component values are tabulated in the computer printouts included with this report. It should be noted that the reported gain of the 15 cm amplifier was significantly lower than the achievable value. This amplifier is less efficient because the diameter of its flashlamp circle is comparable to that of the 20 cm amplifier, in order to accomodate additional fixtures used for testing liquid edge cladding of the laser glass.⁵ Table 1 shows a comparison of the amplifier gains on GEKKO XII-Module and Shiva, and the ratio of

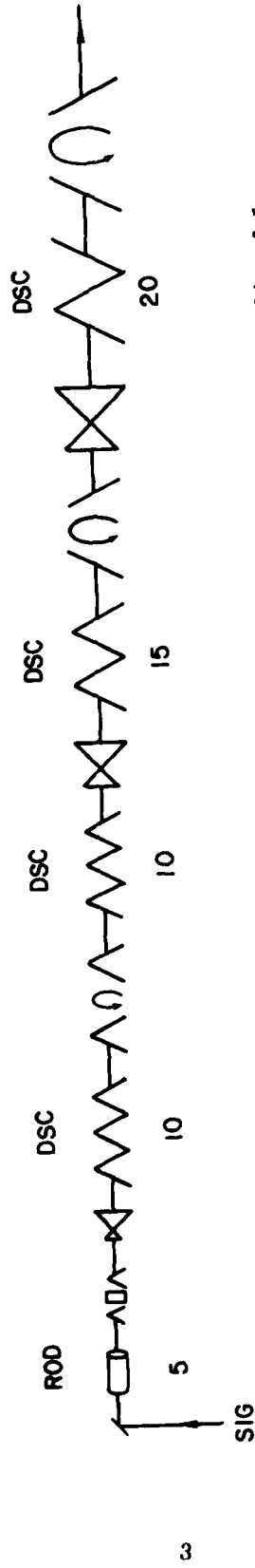


Fig. 1 — Schematic diagram of a single beam line of the Gekko XII Module, as reported in ref. 1

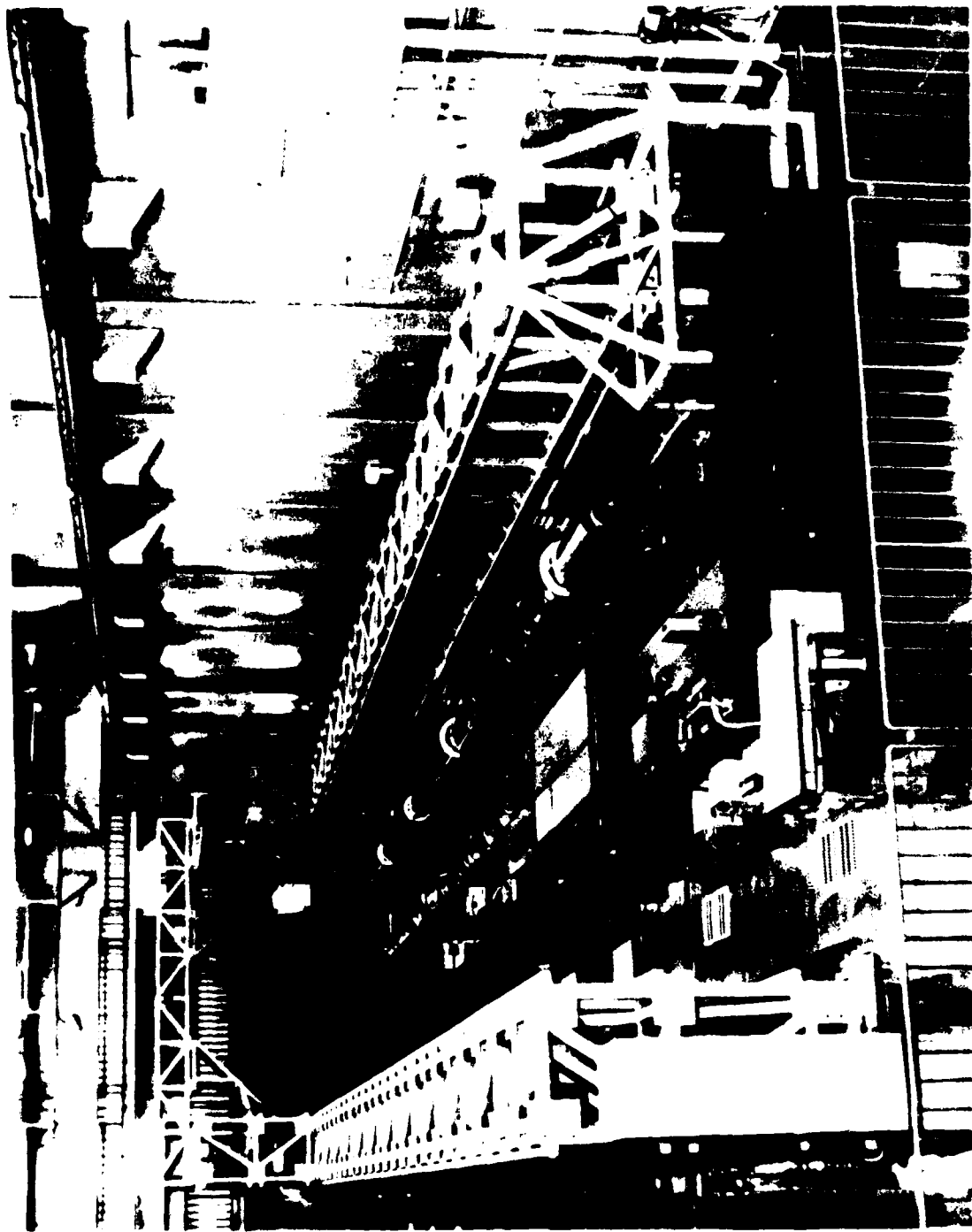


Fig. 2 Recent picture of Gekko XII, showing the oscillator and preamplifier section in the center, and the first test arm on the right hand side.

Table 1: Comparison of Shiva and Gekko XII Disc Amplifiers

<u>Aperture (cm)</u>	<u>Shiva Gain</u>	<u>Gekko Gain</u>	<u>Ratio of Gain Coefficients</u>
10	3.67	8.5	1.65
15	2.61	3.4	1.27
20	1.95	3.2	1.73

the gain coefficients for the two systems. A gain of 3.4 was reported for this amplifier, but a gain of at least 4.88 should be possible if one compares, for example, the 10 cm amplifiers. In computing the Gekko XII short pulse performance we used the reported gain for this amplifier, but in examining nanosecond operation we looked at the performance both with the reported gain and with what should be the achievable gain for the 15 cm disk module.

3. Computer Code

The numerical calculations were carried out using the KARL code⁶ with twenty radial zones and fifty time steps for each optical component. For the pulse incident at the 50 mm rod, the temporal shape was assumed to be Gaussian, while the radial profile was a hyper-Gaussian $\exp\{-(r/r_0)^{12}\}$ with $r_0 = 20$ mm.

The laser amplifiers were modelled by the Avizones-Grotbeck rate equations⁷ with a lower level relaxation term:

$$\begin{aligned} \partial I / \partial z &= \alpha_0 (W_2 - \eta W_1) I - \gamma I \\ \partial W_2 / \partial t &= -(W_2 - \eta W_1) I / (1 + \eta) F_s, & W_2(-\infty) &= 1 \\ \partial W_1 / \partial t &= -\partial W_2 / \partial t - W_1 / T_1, & W_1(-\infty) &= 0 \end{aligned}$$

Here, I is the intensity, W_2 (W_1) is the normalized upper (lower) level population, η is the upper/lower level degeneracy ratio ($\eta = 1$ in all of the runs shown here), F_s is the short pulse saturation flux, and T_1 is the lower level relaxation time. The initial gain coefficient α_0 is found from the relation $\alpha_0 = \gamma + L^{-1} \ln G_0$, where G_0 is the measured small signal gain of the amplifier, L is the active path length, and γ

is the loss coefficient, which models the estimated 1% loss per disc. For most of the runs shown here, we chose $F_s = 2.42 \text{ J/cm}^2$ with $T_1 = 3$ nsec; in Tables VIII and X, however, we used the more optimistic value $F_s = 3.6 \text{ J/cm}^2$ (with $T_1 = 1000$ nsec). In test problems where $\gamma \rightarrow 0$ and $T_1 \gg t(\text{pulse})$, the numerical solutions were found to agree with the Frantz-Nodvik theory to an accuracy better than 1%, even under heavily saturated conditions.

Quantities computed after each component include total power and energy, incremented and total B integrals, peak to average intensity ratios, maximum intensity, and energy density. These are defined in more detail in Table 11. For the nanosecond cases spatial filter transmission was assumed to be unity, as the largest ΔB generated between successive spatial filters was 1.8 in all the cases studied here. For the short pulse cases a LLNL algorithm was used, as discussed below.

4. Short Pulse Test Case

The code was operated to predict GEKKO XII-Module short pulse (50 ps) performance. The spatial filter transmission algorithm used, $T(B) = \{1 + 2 \times 10^{-4} \exp(2\Delta B)\}^{-1}$, was obtained from W.F. Hagen of LLNL, and is the one in use for Shiva and Nova calculations. The generation of low spatial frequency ripples by pinhole truncation and low frequency self-focusing noise amplification was not explicitly included, but was modelled by restricting the spatial profile to have a peak/average intensity ratio greater than 1.6 to 1.

Table III shows a computer listing for the short pulse performance of the original design reported in Ref. 1. Here, a spatial filter was also added at the output of the reported configuration, in order to

Table II: Glossary of Parameters Appearing in the Computer Listings

	APER	THCK	GLIN	ANGL	NO	N2	PNAX	EQU	BIMX	BTMX	P/AV	IMAX	FLUX
	Beam aperture (cm)	Glass thickness (cm)	Small signal gain or transmission	Incidence angle (deg)	Linear refractive index	Nonlinear refractive index (10 ³ x esu)	Peak power (GW)	Total energy (J)	Peak on-axis B increment (rad)	Peak on-axis net B integral (rad)	On-axis flux/average flux	Peak on-axis intensity (GW/cm ²)	On-axis flux (J/cm ²)
DSC	10.00	6x2.43	8.50	56.38	1.504	1.050	.927E02	.464E01	0.165	0.575	1.680	.198E01	.992E01
	(e.g. DSC = Disc amplifier)		(ALD = 2.50, FS = 2.42, ETA = 1.00, T1 = 3.00)										

← Gain coefficient x major diameter
 ← Short pulse saturation flux $h\nu/2\sigma$ (J/cm²)
 ← Upper level degeneracy/lower level degeneracy
 ← Lower level relaxation time (nsec)

highlight the problem with this design. Immediately after the 20 cm disc module, over 4TW/beam of focusable power is available (incremental $B = 1.95$). However, the Faraday rotator package (POL-ROT-POL) immediately following has a very large additional B increment (1.88), and one would expect that much of the power through the final lens would not be focusable. The focusable output is shown on the bottom line of Table III, and the corresponding spatial and temporal profiles are shown in Figure 3. The center of the pulse has clearly been "blown out", resulting in a focusable power of only 2.4TW/beam. It should be noted that the 3.4 TW performance reported in Ref. 3 was measured without the final Faraday rotator package.

Fortunately, this package can be retained in the system without a significant loss of performance. Interchanging the location of Faraday Rotator modules and disk modules in both the 15 and 20 cm sections, one obtains a focusable power of 3.6 TW/beam as shown in Table IV and Figure 4. The reconfigured system has adequate isolation in that a 60% back-reflection would still produce only $1.5\text{J}/\text{cm}^2$ on the 20 cm Faraday rotator.

5. Nanosecond Pulse Performance

The expected nanosecond performance of the reported configuration is summarized in Table V. This design is limited by damage to the AR coated input lens of the 10-15 cm telescope at an output of about 1000 J/beam. This is essentially the same problem as encountered with Shiva at long pulses; i.e., even with the added gain in the phosphate disc amplifiers, the laser is still optimized for short pulses. In this calculation we used a saturation flux of $2.42\text{J}/\text{cm}^2$. Use of a higher saturation flux such as $3.6\text{J}/\text{cm}^2$ would increase the output slightly (ie. $\sim 10\%$).

TABLE III: SHORT (50 psec) PULSE PERFORMANCE OF REPORTED GEKKO SYSTEM

APFA	TIME	GLIN	ANGL	NO	N2	PMAX	EQUT	QTRK	QTRK	P/AV	IMAX	FLUX
SIG	5.00											
880	1K 0.00 (810= 0.43, FS= 2.42)	0.94	56.43	1.504	1.050	-1.00E 01	-5.00E-01	0.000	0.000	1.604	-0.850E-01	-4.29E-02
						-1.33E 02	-6.63E 00	0.213	0.213	1.602	-1.14E 01	-5.68E-01
PBL	5.00	2K 0.00	0.94	56.43	1.507	1.240	-1.25E 02	0.029	0.242	1.602	-1.07E 01	-5.34E-01
PSC	5.00	1K 7.03	0.96	0.00	1.500	1.000	-1.20E 02	0.122	0.364	1.602	-1.03E 01	-5.13E-01
PBL	5.00	2K 0.00	0.94	56.43	1.507	1.240	-1.11E 02	0.026	0.391	1.602	-1.06E 00	-4.02E-02
LWS	5.00	1K 0.00	0.99	0.00	1.507	1.240	-1.11E 02	0.016	0.406	1.602	-0.95E 00	-4.77E-01
SPF	10.00	1K 0.00	1.00	0.00	0.000	0.000	-1.11E 02	0.000	0.406	1.602	-2.39E 00	-1.19E-01
LWS	0.00	1K 0.00	2.99	0.00	1.507	1.240	-1.10E 02	0.004	0.410	1.602	-2.36E 00	-1.18E-01
BSC	10.00	6K 2.42	0.50	56.38	1.504	1.050	-0.27E 02	0.165	0.575	1.600	-1.90E 01	-5.92E-01
						-0.27E 02	-6.64E 01	0.000	0.575	1.600	-1.90E 01	-5.92E-01
PBL	10.00	2K 0.00	0.94	56.43	1.507	1.240	-0.71E 02	0.050	0.626	1.600	-1.06E 01	-9.32E-01
BOT	10.00	1K 0.00	0.98	0.00	1.673	2.100	-0.54E 02	0.046	0.672	1.600	-1.03E 01	-9.13E-01
PBL	10.00	2K 0.00	0.94	56.43	1.507	1.240	-0.80E 02	0.046	0.710	1.600	-1.72E 01	-0.89E-01
BSC	10.00	6K 2.42	0.50	56.38	1.504	1.050	-0.31E 03	1.155	1.873	1.665	-1.34E 02	-6.71E 00
						-0.31E 03	-6.25E 03	0.219	2.092	1.665	-1.32E 02	-6.64E 00
LWS	15.00	1K 0.00	1.00	0.00	0.000	0.000	-0.22E 03	0.000	2.092	1.664	-5.85E 01	-2.94E 00
SPF	15.00	1K 0.00	1.00	0.00	0.000	0.000	-0.22E 03	0.000	2.092	1.664	-5.85E 01	-2.94E 00
LWS	15.00	1K 1.10	0.99	0.00	1.507	1.240	-0.16E 03	0.132	2.224	1.664	-5.79E 01	-2.91E 00
BSC	15.00	6K 3.00	0.40	56.38	1.504	1.050	-1.93E 04	1.800	4.032	1.649	-1.00E 02	-9.06E 00
						-1.93E 04	-9.71E 04	1.800	4.032	1.649	-1.00E 02	-9.06E 00
PBL	15.00	1K 1.10	0.94	56.43	1.507	1.240	-0.18E 04	0.314	4.344	1.649	-1.69E 02	-8.52E 00
BOT	15.00	1K 1.10	0.98	0.00	1.573	2.100	-0.17E 04	0.578	4.918	1.649	-1.66E 02	-8.35E 00
PBL	15.00	1K 1.10	0.94	56.43	1.507	1.240	-0.16E 04	0.290	5.206	1.649	-1.54E 02	-7.85E 00
LWS	15.00	1K 1.10	0.99	0.00	1.507	1.240	-0.16E 04	0.351	5.554	1.649	-1.54E 02	-7.77E 00
SPF	20.00	1K 0.00	1.00	0.00	0.000	0.000	-0.14E 04	0.000	5.554	1.617	-1.22E 01	-6.06E 00
LWS	20.00	1K 1.50	0.99	0.00	1.507	1.240	-0.14E 04	0.222	5.774	1.617	-1.22E 01	-6.06E 00
BSC	20.00	6K 3.00	0.20	56.38	1.504	1.050	-0.41E 04	1.732	7.459	1.601	-2.10E 02	-1.15E 01
						-0.41E 04	-2.26E 03	1.732	7.459	1.601	-2.10E 02	-1.15E 01
PBL	20.00	1K 1.50	0.94	56.43	1.507	1.240	-0.39E 04	0.500	7.937	1.601	-1.97E 02	-1.00E 01
BOT	20.00	1K 1.50	0.98	0.00	1.673	2.100	-0.38E 04	0.920	8.876	1.601	-1.93E 02	-1.00E 01
PBL	20.00	1K 1.50	0.94	56.43	1.507	1.240	-0.36E 04	0.461	9.287	1.601	-1.82E 02	-9.99E 00
LWS	20.00	1K 1.50	0.99	0.00	1.507	1.240	-0.35E 04	0.558	9.833	1.601	-1.80E 02	-9.89E 00
SPF	20.00	1K 0.00	1.00	0.00	0.000	0.000	-0.27E 04	0.000	9.833	1.490	-1.16E 02	-7.14E 00

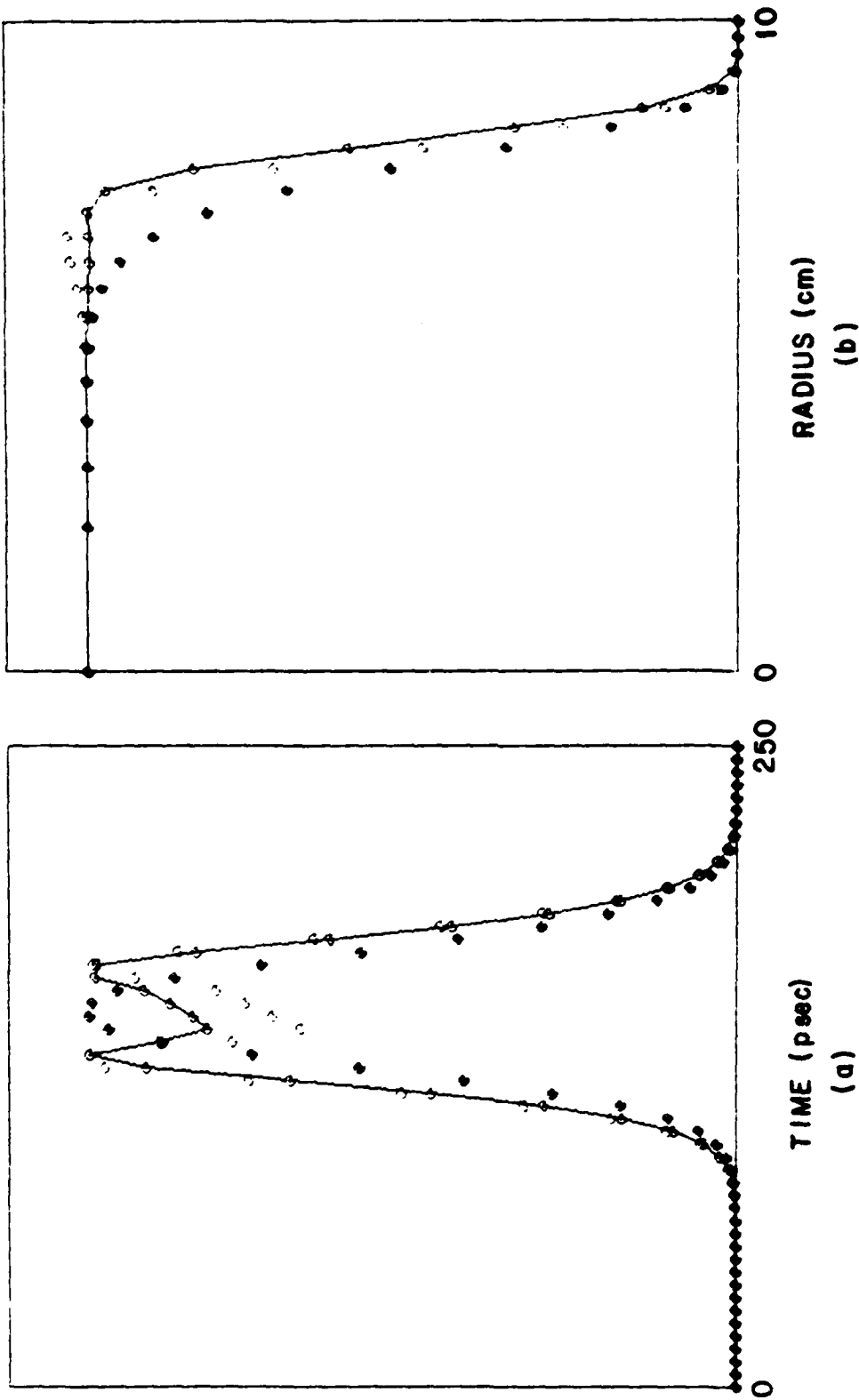


Fig. 3 -- Temporal (3a) and spatial (3b) profiles and the output of the reported configuration with a 50 psec input pulse. In (3a): $\circ\circ\circ\circ\circ$ = Power, $\bullet\bullet\bullet\bullet\bullet$ = Intensity on axis, and $\square\square\square\square\square$ = Total nonlinear phase distortion (B integral) on axis. In (3b): $\circ\circ\circ\circ\circ$ = Flux, $\bullet\bullet\bullet\bullet\bullet$ = Intensity at the time of peak power, and $\square\square\square\square\square$ = Total nonlinear phase distortion at the time of peak power.

TABLE IV: SHORT (50 psec) PERFORMANCE OF RECONFIGURED SYSTEM

TE= 0.050 WL= 1.053

SIG	APER	TMCR	GLIM	ANGL	NO	M2	PMAK	EQUT	BIEM	BTME	P/AV	INDX	PLUR
SIG	5.00												
R00	5.00	1X 0.00	13.40	0.00	1.504	1.050			0.000	0.000	1.604	.050E-01	.029E-02
		(ALD= 0.43, FS= 2.42, EIA= 1.00, T1= 3.00)							0.213	0.213	1.602	.114E 01	.500E-01
P0L	5.00	2X 0.00	0.94	56.43	1.507	1.240			0.029	0.242	1.607	.107E 01	.534E-01
P0C	5.00	1X 7.00	3.96	0.00	1.500	1.000			0.122	0.364	1.602	.103E 01	.513E-01
P0L	5.00	2X 0.00	0.94	56.43	1.507	1.240			0.024	0.391	1.602	.064E 00	.402E-01
LWS	5.00	1X 0.00	3.99	0.00	1.507	1.240			0.016	0.406	1.602	.055E 00	.477E-01
SPF	10.00	1X 0.00	1.00	0.00	0.000	0.000			0.000	0.406	1.602	.239E 00	.119E-01
LWS	10.00	1X 0.00	0.99	0.00	1.507	1.240			0.004	0.410	1.602	.236E 00	.110E-01
BSC	10.00	4X 2.40	0.50	56.38	1.504	1.050			0.165	0.575	1.600	.190E 01	.992E-01
		(ALD= 2.50, FS= 2.42, EIA= 1.00, T1= 3.00)							0.050	0.626	1.600	.100E 01	.937E-01
P0L	10.00	2X 0.00	0.94	56.43	1.507	1.240			0.046	0.672	1.600	.103E 01	.913E-01
R0Y	10.00	1X 0.00	0.98	0.00	1.673	2.100			0.046	0.718	1.600	.172E 01	.059E-01
P0L	10.00	2X 0.00	0.94	56.43	1.507	1.240			1.155	1.073	1.665	.134E 02	.631E 00
BSC	10.00	4X 2.40	0.50	56.38	1.504	1.050			0.219	2.092	1.665	.132E 02	.644E 00
		(ALD= 2.50, FS= 2.42, EIA= 1.00, T1= 3.00)							0.000	2.092	1.665	.505E 01	.294E 00
LWS	10.00	1X 0.00	0.99	0.00	1.507	1.240			0.132	2.224	1.665	.579E 01	.291E 00
SPF	15.00	1X 0.00	1.00	0.00	0.000	0.000			0.101	2.375	1.665	.544E 01	.274E 00
LWS	15.00	1X 1.10	0.99	0.00	1.507	1.240			0.186	2.511	1.665	.533E 01	.240E 00
P0L	15.00	1X 1.10	0.94	56.43	1.507	1.240			0.093	2.604	1.665	.501E 01	.257E 00
BSC	15.00	4X 3.00	3.40	56.38	1.504	1.050			1.575	4.100	1.651	.157E 02	.793E 00
		(ALD= 2.55, FS= 2.42, EIA= 1.00, T1= 3.00)							0.354	4.532	1.651	.150E 02	.705E 00
LWS	15.00	1X 1.10	0.99	0.00	1.507	1.240			0.000	4.532	1.646	.054E 01	.437E 00
SPF	20.00	1X 0.00	1.00	0.00	0.000	0.000			0.262	4.793	1.646	.046E 01	.432E 00
LWS	20.00	1X 1.50	0.99	0.00	1.507	1.240			0.202	4.994	1.646	.079E 01	.404E 00
P0L	20.00	1X 1.50	0.94	56.43	1.507	1.240			0.370	5.362	1.646	.077E 01	.390E 00
R0Y	20.00	1X 1.50	0.98	0.00	1.673	2.100			0.186	5.547	1.646	.073E 01	.374E 00
P0L	20.00	1X 1.50	0.94	56.43	1.507	1.240			1.745	7.204	1.629	.217E 02	.180E 01
BSC	20.00	3X 3.20	3.20	56.38	1.504	1.050			0.653	7.923	1.629	.211E 02	.107E 01
		(ALD= 3.96, FS= 2.42, EIA= 1.00, T1= 3.00)							0.000	7.923	1.601	.170E 02	.959E 00
LWS	20.00	1X 1.50	0.99	0.00	1.507	1.240			0.206	8.092	1.601	.157E 02	.793E 00
SPF	20.00	1X 0.00	1.00	0.00	0.000	0.000			0.358	8.411	1.601	.150E 02	.705E 00

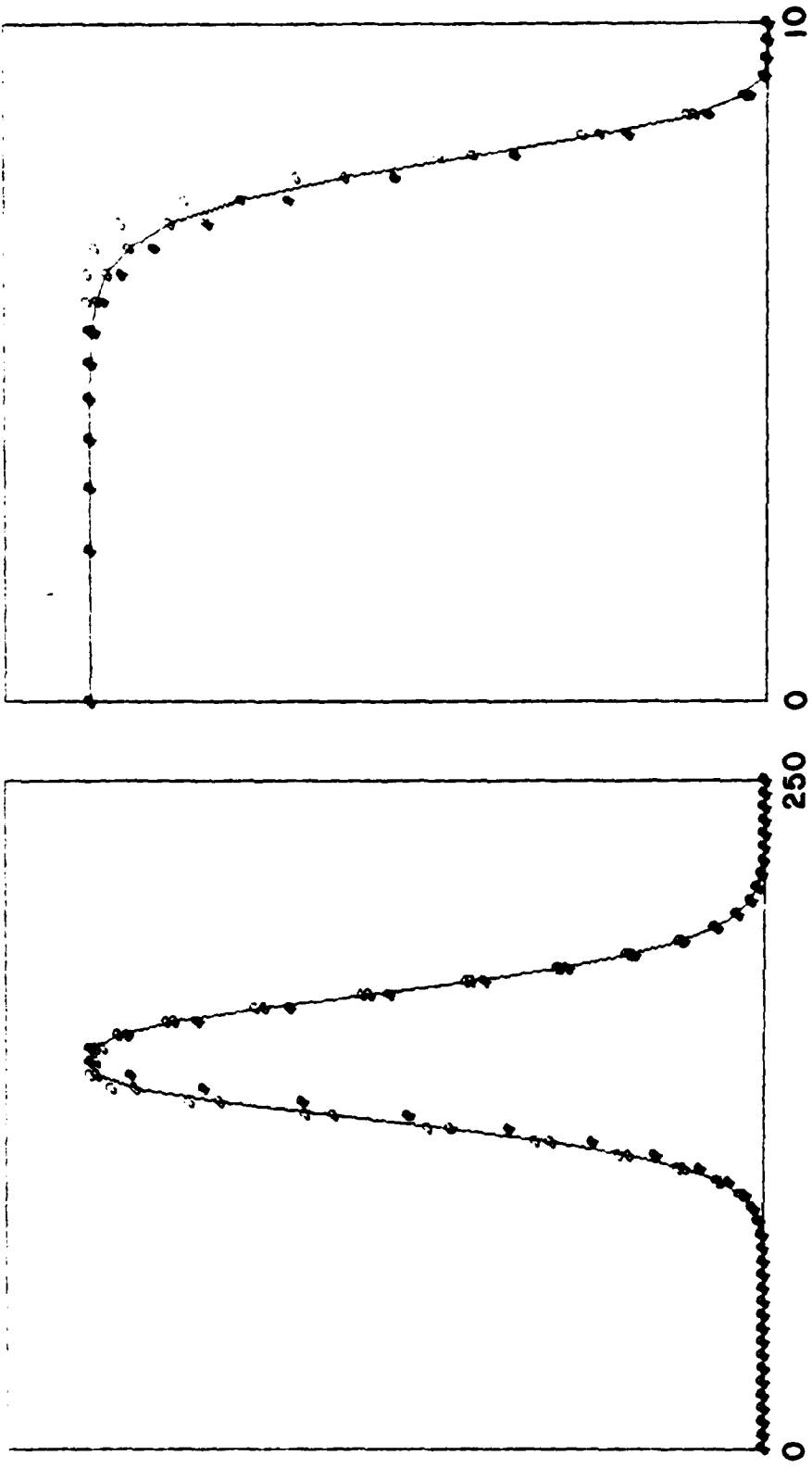


Fig. 4 -- Temporal (4a) and spatial (4b) profiles at the output of the reconfigured system with a 50 psec input pulse. The curves have the same meaning as those in Figs. (3a, b).

TABLE V: NANOSECOND PERFORMANCE OF REPORTED GEKKO SYSTEM

TE: 1.000 microns WL: 1.053 μ

SIG	APER	THICK	GLIN	ANGL	NO	NZ	PHAS	EQUT	DIRK	STOR	P/AV	TERR	PLUD
516	5.00						.129E 01	.129E 01	0.000	0.000	1.000	.107E 00	.107E 00
999	5.00	1230.00	13.50	0.00	1.504	1.050	.137E 02	.130E 02	0.230	0.220	1.049	.119E 01	.110E 01
		(ALO=0.63)	FS=2.62	ETA=1.00	TI=3.00								
900	5.00	28 0.00	0.94	56.53	1.507	1.240	.129E 02	.130E 02	0.020	0.207	1.040	.100E 01	.100E 01
906	5.00	18 7.00	0.96	0.00	1.500	1.000	.124E 02	.125E 02	0.126	0.300	1.040	.100E 01	.100E 01
908	5.00	28 0.00	0.94	56.53	1.507	1.240	.116E 02	.117E 02	0.026	0.416	1.040	.076E 00	.085E 00
105	5.00	18 0.00	0.99	0.00	1.507	1.240	.119E 02	.116E 02	0.016	0.432	1.040	.066E 00	.079E 00
105	10.00	18 0.00	0.99	0.00	1.507	1.240	.116E 02	.115E 02	0.006	0.436	1.040	.239E 00	.241E 00
050	10.00	68 2.50	0.50	56.30	1.504	1.050	.012E 02	.010E 02	0.152	0.507	1.016	.107E 01	.100E 01
		(ALO=2.50)	FS=2.62	ETA=1.00	TI=3.00								
000	10.00	28 0.00	0.94	56.53	1.507	1.240	.104E 02	.105E 02	0.042	0.620	1.016	.137E 01	.130E 01
007	10.00	18 0.00	0.90	0.00	1.507	1.073	.103E 02	.105E 02	0.070	0.659	1.016	.150E 01	.155E 01
008	10.00	28 0.00	0.94	56.53	1.507	1.240	.104E 02	.100E 02	0.030	0.700	1.016	.145E 01	.140E 01
050	10.00	68 2.50	0.50	56.30	1.504	1.050	.107E 03	.116E 03	0.070	1.357	1.026	.000E 01	.010E 01
		(ALO=2.50)	FS=2.62	ETA=1.00	TI=3.00								
105	10.00	18 0.00	0.99	0.00	1.507	1.240	.104E 03	.111E 03	0.099	1.447	1.026	.500E 01	.600E 01
105	15.00	18 1.10	0.99	0.00	1.507	1.240	.103E 03	.100E 03	0.040	1.505	1.026	.203E 01	.266E 01
050	15.00	48 3.00	3.00	52.30	1.508	1.050	.020E 03	.020E 03	0.076	2.123	1.075	.570E 01	.500E 01
		(ALO=2.50)	FS=2.62	ETA=1.00	TI=3.00								
000	15.00	18 1.10	0.94	56.53	1.507	1.240	.020E 03	.037E 03	0.100	2.200	1.075	.530E 01	.520E 01
007	15.00	18 1.10	0.90	0.00	1.507	1.073	.036E 03	.025E 03	0.103	2.305	1.075	.529E 01	.521E 01
008	15.00	28 1.10	0.94	56.53	1.507	1.240	.020E 03	.020E 03	0.092	2.447	1.075	.693E 01	.600E 01
105	15.00	18 1.10	0.99	0.00	1.507	1.240	.020E 03	.020E 03	0.111	2.952	1.075	.609E 01	.695E 01
105	20.00	18 1.50	0.99	0.00	1.507	1.240	.020E 03	.020E 03	0.004	2.632	1.075	.272E 01	.270E 01
050	20.00	38 3.20	3.20	56.30	1.504	1.050	.122E 04	.122E 04	0.552	3.120	1.031	.570E 01	.600E 01
		(ALO=3.00)	FS=2.62	ETA=1.00	TI=3.00								
000	20.00	18 1.50	0.94	56.53	1.507	1.240	.110E 04	.110E 04	0.130	3.200	1.031	.500E 01	.520E 01
007	20.00	18 1.50	0.90	0.00	1.507	1.073	.110E 04	.110E 04	0.253	3.450	1.031	.530E 01	.510E 01
008	20.00	28 1.50	0.94	56.53	1.507	1.240	.106E 04	.106E 04	0.127	3.505	1.031	.501E 01	.602E 01
105	20.00	18 1.50	0.99	0.00	1.507	1.240	.104E 04	.104E 04	0.150	3.600	1.031	.600E 01	.677E 01

The performance can be improved somewhat by the use of uncoated input lenses to the spatial filters, and the interchange of disc and Faraday Rotator modules. Table VI summarizes this case for a saturation flux of 2.42 J/cm^2 . One can now obtain 1300 Joules/beam with a maximum allowable backreflection of 65% (assuming a 5 J/cm^2 damage threshold⁹ at the AR coated Faraday rotator). Note, however, that the highest fluxes are still encountered on the same 10-15 cm spatial filter lens, so we have not removed the bottleneck.

Increasing the gain of the 15 cm disc amplifier from 3.4 to 4.88 will also improve the situation somewhat, as shown in Table VII for a 2.42 J/cm^2 saturation flux. The output increases to 1500 J/beam, and the bottlenecking is further reduced. If a saturation flux of 3.6 J/cm^2 is assumed (Table VIII), even less bottlenecking is evident, and an output of 1710J/beam is obtained. The allowable backreflection for these two cases is 60% and 45%, respectively.

To increase the output above this level, it is necessary to either increase the gain of the high energy section or decrease the losses in this section. One way to decrease the losses is to replace the uncoated spatial filter lenses with lenses fabricated of a phase separable glass such as Hoya ARG-2. Tables IX and X show the expected performance if this is done for saturation fluxes of 2.42 and 3.6 J/cm^2 , respectively. Outputs of 1800J/beam and 2060J/beam were obtained for the two cases, and the allowable backreflections were 48% and 35%. Note, however, that moderately high fluxes were incident on the AR-coated Faraday Rotator glass; i.e., 4.51 J/cm^2 and 5.12 J/cm^2 .

The alternate strategy (ie. increase of the gain) was examined by modeling the performance with an additional 20 cm amplifier. Table XI and Fig. 5

TABLE VII: EFFECT OF HIGHER GAIN 15cm AMPLIFIER

TYPE	INCL	ANGLE	NO	RZ	PMIX	EOUT	DIRN	P/AV	INCR	FLOR
900	9.00				.500E 01	.500E 01	0.000	1.000	.420E 00	.450E 00
900	10.00	1.00	1.500	1.000	.500E 02	.500E 02	0.150	1.500	.310E 01	.310E 01
		(1.00- 2.50, 75- 2.50, 71- 3.00)								
900	5.00	2H 0.00	2.25	1.507	.350E 02	.350E 02	0.037	1.535	.292E 01	.292E 01
900	9.00	1H 7.00	0.96	1.000	.500E 02	.500E 02	0.333	1.000	.200E 01	.200E 01
900	5.00	2H 0.00	0.96	1.507	.320E 02	.320E 02	0.071	1.230	.263E 01	.270E 01
105	9.00	1H 0.00	0.99	1.000	.310E 02	.320E 02	0.063	1.201	.200E 01	.207E 01
105	10.00	1H 0.00	0.99	1.507	.310E 02	.320E 02	0.011	1.291	.445E 00	.461E 00
900	10.00	6H 2.50	0.50	1.504	.100E 03	.107E 03	0.301	1.536	.362E 01	.365E 01
		(1.00- 2.50, 75- 2.50, 71- 3.00)								
900	10.00	2H 0.00	0.96	1.507	.170E 03	.170E 03	0.092	1.710	.101E 01	.090E 01
900	10.00	1H 0.00	0.98	1.000	.160E 03	.172E 03	0.085	1.000	.320E 01	.320E 01
900	10.00	2H 0.00	0.96	1.507	.150E 03	.162E 03	0.095	1.005	.316E 01	.316E 01
900	10.00	6H 2.50	0.50	1.504	.100E 03	.110E 03	1.203	2.500	.500E 01	.500E 01
		(1.00- 2.50, 75- 2.50, 71- 3.00)								
105	10.00	1H 0.00	0.93	1.000	.071E 03	.083E 03	0.121	3.045	.009E 01	.004E 01
105	10.00	1H 1.10	0.92	1.000	.060E 03	.070E 03	0.083	3.122	.291E 01	.291E 01
900	10.00	1H 1.10	0.96	1.507	.030E 03	.030E 03	0.060	3.100	.307E 01	.300E 01
900	10.00	1H 1.10	0.98	1.000	.030E 03	.030E 03	0.126	3.200	.160E 01	.150E 01
900	10.00	1H 1.12	0.94	1.507	.004E 03	.014E 03	0.053	3.252	.330E 01	.337E 01
900	10.00	6H 2.50	0.50	1.504	.102E 04	.102E 04	0.907	0.007	.000E 01	.000E 01
		(1.00- 2.50, 75- 2.50, 71- 3.00)								
105	10.00	1H 1.10	0.93	1.000	.051E 03	.051E 03	0.166	4.170	.102E 01	.100E 01
105	10.00	1H 1.50	0.99	1.507	.041E 03	.041E 03	0.135	4.214	.030E 01	.030E 01
900	10.00	1H 1.50	0.94	1.507	.030E 03	.030E 03	0.104	4.204	.010E 01	.010E 01
900	10.00	1H 1.50	0.90	1.000	.000E 03	.000E 03	0.101	4.502	.001E 01	.001E 01
900	10.00	1H 1.50	0.94	1.507	.010E 03	.010E 03	0.066	4.576	.077E 01	.077E 01
900	10.00	6H 2.50	0.50	1.504	.100E 04	.100E 04	0.733	3.000	.100E 01	.100E 01
		(1.00- 2.50, 75- 2.50, 71- 3.00)								
105	10.00	1H 1.52	0.93	1.000	.125E 03	.125E 03	0.180	5.000	.100E 01	.100E 01

TABLE X: EFFECT OF HIGHER SATURATION FLUX

TE= 1.000 ML= 1.053

APER	TRCE	GAIR	ANGL	NO	N2	PMAX	EQUT	QBK	ETBK	P/AV	100K	FLUX
5.00												
5.00	1X 10.00	13.40	0.00	1.504	1.050			0.000	0.000	1.404	.203E 00	.203E 00
	(ALD= 0.43, FS= 3.00, ETA= 1.00, TI= 0.00000)											
5.00	2X 0.00	0.94	56.43	1.507	1.240			0.067	0.647	1.424	.249E 01	.249E 01
5.00	1X 7.00	0.94	0.00	1.500	1.000			0.205	0.931	1.426	.239E 01	.240E 01
5.00	2X 0.00	0.94	56.43	1.507	1.240			0.061	0.992	1.426	.229E 01	.226E 01
5.00	1X 0.00	0.99	0.00	1.507	1.240			0.037	1.029	1.426	.222E 01	.223E 01
10.00	1X 0.00	0.99	0.00	1.507	1.240			0.009	1.030	1.426	.551E 00	.553E 00
10.00	4X 2.40	0.50	56.30	1.504	1.050			0.329	1.367	1.501	.351E 01	.349E 01
	(ALD= 2.50, FS= 3.00, ETA= 1.00, TI= 0.00000)											
10.00	2X 0.00	0.94	56.43	1.507	1.240			0.009	1.454	1.501	.330E 01	.320E 01
10.00	1X 0.00	0.90	0.00	1.673	2.100			0.002	1.534	1.501	.323E 01	.321E 01
10.00	2X 0.00	0.94	56.43	1.507	1.240			0.002	1.614	1.501	.304E 01	.302E 01
10.00	4X 2.40	0.50	56.30	1.504	1.050			1.291	2.016	1.402	.100E 02	.100E 02
	(ALD= 2.50, FS= 3.00, ETA= 1.00, TI= 0.00000)											
10.00	1X 0.00	0.99	0.00	1.507	1.240			0.170	2.971	1.402	.107E 02	.105E 02
15.00	1X 1.10	0.99	0.00	1.507	1.240			0.107	3.005	1.402	.472E 01	.463E 01
15.00	1X 1.10	0.94	56.43	1.507	1.240			0.003	3.137	1.402	.444E 01	.435E 01
15.00	1X 1.10	0.90	0.00	1.673	2.100			0.152	3.270	1.402	.435E 01	.426E 01
15.00	1X 1.10	0.94	56.43	1.507	1.240			0.076	3.336	1.402	.409E 01	.401E 01
15.00	4X 3.00	4.00	56.30	1.504	1.050			1.172	4.337	1.417	.105E 02	.900E 01
	(ALD= 3.20, FS= 3.00, ETA= 1.00, TI= 0.00000)											
15.00	1X 1.10	0.99	0.00	1.507	1.240			0.236	4.526	1.417	.104E 02	.970E 01
20.00	1X 1.50	0.99	0.00	1.507	1.240			0.100	4.669	1.417	.579E 01	.545E 01
20.00	1X 1.50	0.94	56.43	1.507	1.240			0.130	4.700	1.417	.544E 01	.512E 01
20.00	1X 1.50	0.90	0.00	1.673	2.100			0.254	4.902	1.417	.534E 01	.502E 01
20.00	1X 1.50	0.94	56.43	1.507	1.240			0.127	5.004	1.417	.501E 01	.472E 01
20.00	3X 3.20	3.20	56.30	1.504	1.050			0.995	5.905	1.375	.101E 02	.909E 01
	(ALD= 3.90, FS= 3.00, ETA= 1.00, TI= 0.00000)											
20.00	1X 1.50	0.99	0.00	1.507	1.240			0.311	6.145	1.375	.100E 02	.900E 01

TABLE XI: RECONFIGURED SYSTEM WITH HIGHER GAIN 15cm AMPLIFIER, UNCOATED INPUT LENSES,
AND AN ADDITIONAL 20cm AMPLIFIER

TI = 1.00 WL = 1.053

APER	TIME	GLIM	ANGL	NO	M2	PMAX	EOUT	DIRX	DIRY	P/AV	IRMX	FLUX
5.00						.500E 01	.500E 01	0.000	0.000	1.684	.429E 00	.429E 00
5.00	1X 3.00	13.40	0.00	1.504	1.050	.300E 02	.302E 02	0.759	0.759	1.595	.310E 01	.310E 01
	(ALD= 0.43, FS= 2.62, ETA= 1.00, TI= 3.00)											
5.00	2X 3.00	0.94	56.43	1.507	1.240	.350E 02	.368E 02	0.079	0.079	1.595	.292E 01	.292E 01
5.00	1X 3.00	0.94	0.00	1.500	1.000	.343E 02	.353E 02	0.333	0.333	1.460	.200E 01	.200E 01
5.00	2X 0.80	0.94	56.43	1.507	1.240	.323E 02	.332E 02	0.071	0.071	1.595	.263E 01	.270E 01
5.00	1X 0.80	0.99	0.00	1.507	1.240	.319E 02	.329E 02	0.043	0.043	1.595	.260E 01	.267E 01
10.00	1X 0.80	0.99	0.60	1.507	1.240	.316E 02	.326E 02	0.011	0.011	1.595	.645E 00	.645E 00
10.00	6X 2.40	0.50	56.38	1.504	1.050	.103E 03	.107E 03	0.361	0.361	1.536	.362E 01	.365E 01
	(ALD= 2.50, FS= 2.62, ETA= 1.00, TI= 3.00)											
10.00	2X 0.80	0.94	56.43	1.507	1.240	.172E 03	.176E 03	0.092	0.092	1.536	.341E 01	.343E 01
10.00	1X 0.80	0.98	0.00	1.673	2.100	.168E 03	.172E 03	0.085	0.085	1.536	.339E 01	.337E 01
10.00	2X 0.80	0.94	56.43	1.507	1.240	.158E 03	.162E 03	0.085	0.085	1.536	.334E 01	.334E 01
10.00	6X 2.40	0.50	56.38	1.504	1.050	.505E 03	.518E 03	1.203	1.203	1.436	.952E 01	.947E 01
	(ALD= 2.50, FS= 2.62, ETA= 1.00, TI= 3.00)											
10.00	1X 0.80	0.93	0.00	1.451	0.950	.471E 03	.483E 03	0.121	0.121	1.436	.889E 01	.884E 01
15.00	1X 1.10	0.99	0.00	1.507	1.240	.466E 03	.478E 03	0.089	0.089	1.436	.391E 01	.389E 01
15.00	1X 1.10	0.94	56.43	1.507	1.240	.430E 03	.450E 03	0.068	0.068	1.436	.347E 01	.345E 01
15.00	1X 1.10	0.98	0.00	1.673	2.100	.430E 03	.441E 03	0.126	0.126	1.436	.360E 01	.358E 01
15.00	1X 1.10	0.94	56.43	1.507	1.240	.404E 03	.414E 03	0.083	0.083	1.436	.339E 01	.337E 01
15.00	6X 3.00	4.00	56.38	1.504	1.050	.102E 04	.102E 04	4.042	4.042	1.375	.830E 01	.791E 01
	(ALD= 3.20, FS= 2.62, ETA= 1.00, TI= 3.00)											
15.00	1X 1.10	0.93	0.00	1.451	0.950	.451E 03	.460E 03	0.114	0.114	1.375	.702E 01	.700E 01
20.00	1X 1.50	0.99	0.00	1.507	1.240	.991E 03	.938E 03	0.135	0.135	1.375	.636E 01	.611E 01
20.00	1X 1.50	0.94	56.43	1.507	1.240	.885E 03	.882E 03	0.104	0.104	1.375	.610E 01	.604E 01
20.00	1X 1.50	0.94	0.00	1.673	2.100	.867E 03	.864E 03	0.191	0.191	1.375	.602E 01	.590E 01
20.00	1X 1.50	0.94	56.43	1.507	1.240	.815E 03	.812E 03	0.096	0.096	1.375	.371E 01	.356E 01
20.00	3X 3.00	3.20	56.38	1.504	1.050	.166E 04	.160E 04	0.743	0.743	1.337	.759E 01	.680E 01
	(ALD= 3.96, FS= 2.62, ETA= 1.00, TI= 3.00)											
20.00	3X 3.00	3.20	56.38	1.504	1.050	.275E 04	.261E 04	1.334	1.334	1.298	.125E 02	.108E 02
	(ALD= 3.96, FS= 2.62, ETA= 1.00, TI= 3.00)											
20.00	1X 1.50	0.93	0.00	1.451	0.950	.257E 04	.244E 04	0.296	0.296	1.298	.612E 01	.610E 01

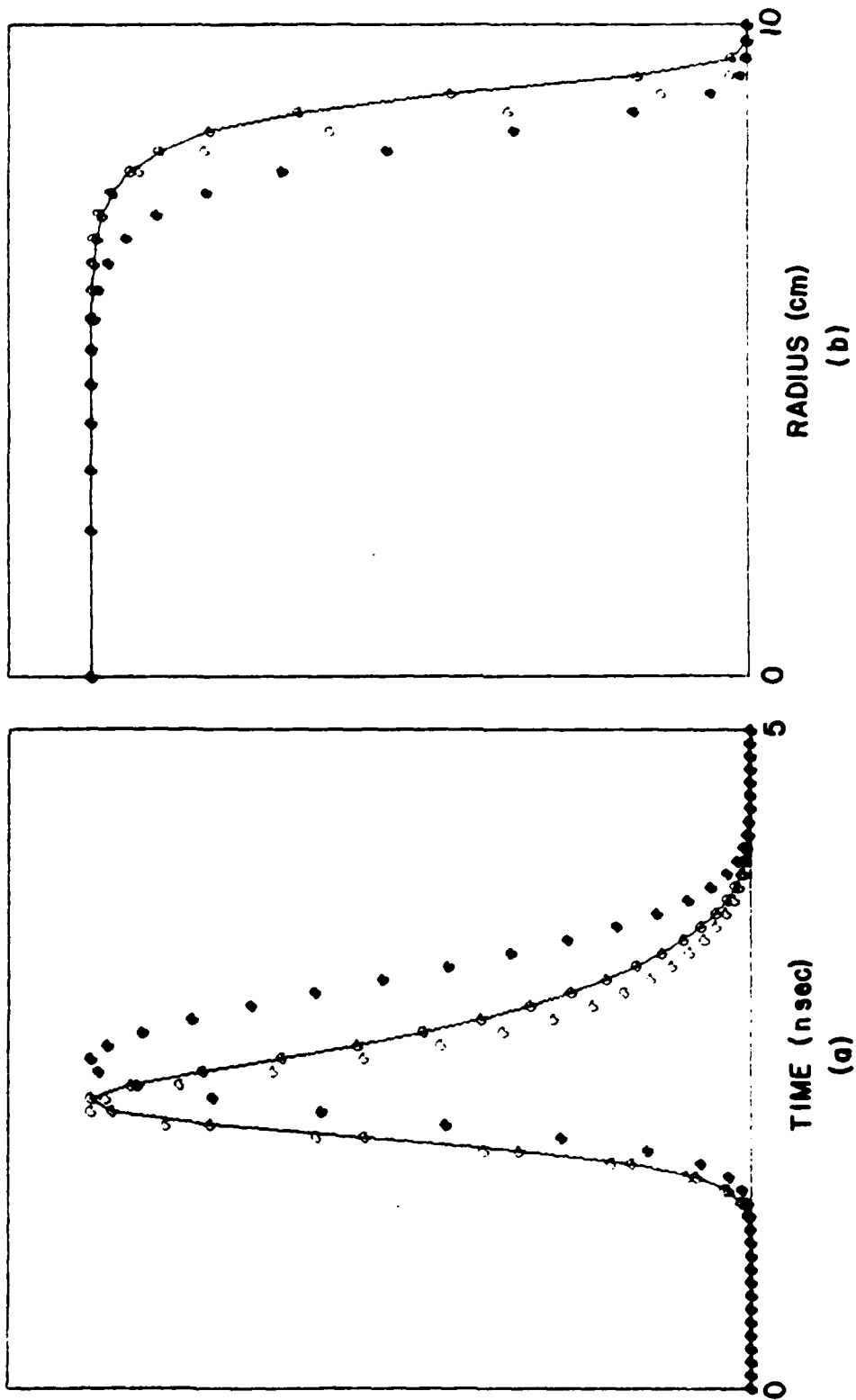


Fig. 5 — Temporal (5a) and spatial (5b) profiles at the output of the system described in Table XI with a nanosecond input pulse. The curves have the same meaning as those in Figs. (3a, b).

show the results for a case where this was done using uncoated spatial filter input lenses and a saturation flux of 2.42 J/cm^2 . An output of 2500 Joules/beam was obtained from the laser at the same total B integral as found in the previous cases at 1800 and 2060 J/beam outputs; moreover, the flux on the Faraday Rotator was reduced to 3.86 J/cm^2 . The allowable backreflection in this configuration was 25%. With a higher saturation flux or ARG-2 lenses, the output energy would not increase because the output lens is now the weak link; however, these expedients could be used to reduce the B integral and the flux on earlier components to slightly lower values.

6. Summary

The GEKKO XII-Module phosphate laser system appears capable in the reported configuration of substantially exceeding the Shiva performance. In fact, it appears that it would closely match the per beam performance of Argus (2.5 TW short pulse, 1000J in a nanosecond pulse) with much lower cost because of the smaller number of amplifiers.

The reported configuration, however, does not appear to represent the most cost effective strategy for either short or long pulses. A different configuration of the same elements and a different type of input spatial filter lens appears capable of increasing the output by at least 50%. Adding an additional twenty centimeter amplifier to each arm appears to be a relatively cost effective strategy for boosting the output in nanosecond pulses to 2.5 kJ per beam. Although these designs would provide adequate isolation for most single beam experiments, they would probably have to be supplemented by plasma shutters⁹ at the outputs in multi beam configurations, where backreflection could be a serious problem.

If Shiva were retrofitted with phosphate glass, it should be capable of 35kJ or more with the present amplifiers, and 50kJ with an additional 20cm phosphate disc amplifier per beam.

7. Acknowledgments

The authors wish to thank Prof. Y. Kato of Osaka University for several helpful suggestions and comments.

References

1. Y. Kato, S. Nakai and C. Yamanaka, Proceedings of the IAEA Technical Committee on Advances in Inertial Confinement Systems; ed. by C. Yamanaka (Institute of Laser Engineering, Osaka University, 1980) p. 59
2. C. Yamanaka, Topical Meeting on Inertial Confinement Fusion (San Diego, CA, 26-28 February, 1980) paper TUA3.
3. Y. Kato, K. Yoshida, J. Kuroda and C. Yamanaka, Appl. Phys. Lett (in print).
4. Laser Program Annual Report - 1978, Lawrence Livermore Laboratory UCRL-50021-78 (Vol. 1, Sec. 2).
5. Y. Kato, private communication.
6. J.M. McMahon, R.H. Lehmborg and S.E. Bodner, Technical Digest: Inertial Confinement Fusion, published by Optical Society of America, Paper TuB3-1 (1978).
7. P.V. Avizones and R.L. Grotbeck, J. Appl. Phys. 37, 687 (1966).
8. This value was obtained from the expression $h\nu/2\sigma$ and the measured LGH-7 cross section $\sigma = 3.9 \times 10^{-20} \text{ cm}^2$. (S.E. Stokowski, R.A. Saroyan and M.J. Weber; Nd-Doped Laser Glass Spectroscopic and Physical Properties, Lawrence Livermore Laboratory report prepared for USDOE under contract No. W-7405-Eng-48; November 1978). For a pulsewidth of 1 nsec and a lower level relaxation time $T_1 = 3 \text{ nsec}$, the effective saturation flux is approximately 2.6 J/cm^2 .
9. Laser Program Annual Report-1979, Lawrence Livermore National Laboratory UCRL-50021-79 (Vol. 1, Sec. 2)

DISTRIBUTION LIST

USDOE (50 copies)

P.O. Box 62

Oak Ridge, TN 37830

National Technical Information Service (24 copies)

U.S. Department of Commerce

5285 Port Royal Road

Springfield, VA 22161

NRL, Code 2628 (35 copies)

NRL, Code 4730 (100 copies)

NRL, Code 4700 (25 copies)

USDOE (8 copies)

Office of Inertial Fusion

Washington, D.C. 20545

Attn: Dr. G. Canavan

Dr. R. Schriever

Dr. S. Kahalas

Dr. T. Godlove

Dr. K. Gilbert

Dr. S. Barish

Rutherford Laboratory

Chilton, Didcot

Oxon OX11 0QX

England

Attn: Dr. M. Key

Sandia Laboratory

Albuquerque, NM 87115

Attn: Dr. J. Yonas

Lawrence Livermore Laboratory

P.O. Box 808

Livermore, CA 94550

Attn: Dr. J. Lindl, L32

Dr. L. Coleman

Dr. J. Nuckolls

Dr. J. Emmett

Dr. J. Hunt

Dr. W. Simmons

Dr. R. Speck

Dr. J. Holzrichter

Institute for Laser Engineering

Osaka University

Suita Osaka, 565

JAPAN

Attn: Dr. C. Yamanaka

Dr. Y. Kato

Schaefer Assoc.

1901 N. Fort Myer Drive

Arlington, VA 22211

Attn: Dr. E. Gerry

Los Alamos Scientific Laboratory

Los Alamos, NM 87545

Attn: Dr. J. Kindel

Dr. S. Rockwood

Science Applications Inc.

Crystal City, VA 22102

Attn: Dr. W. Sooy

University of Rochester

Laboratory for Laser Energetics

Rochester, NY 14627

Attn: Dr. J. Soures

Dr. W. Seka

National Research Council

Division of Physics

100 Sussex Drive

Ottawa K1A-0R6, Canada

**EN
DAT**